Localization and delocalization of an electron in biased and unbiased quantum wells driven by a mono- and bichromatic laser field

Yuri Dakhnovskii
Department of Chemistry, Carnegie Mellon University, 4400 Fifth Avenue, Pittsburgh, Pennsylvania 15213

Raanan Bavli and Horia Metiu
Department of Chemistry, University of California, Santa Barbara, California 93106
(Received 11 September 1995)

Localization (delocalization) of an electron driven by laser in a biased quantum well is considered. The initially trapped electron can be delocalized by the field if the bias energy is close but not equal to an integer number of a photon energy. When the bias energy is exactly equal to an integer number of photon quanta, dynamical localization occurs. A general analytical solution for a population difference is obtained. When the electron is driven by a bichromatic field, localization regions are strongly dependent on the field incommensurability. The topology of localization exhibits stable and unstable regions originating from nonanalytical behavior of the population with respect to the small incommensurability. This phenomenon resembles phase-transition instabilities in the solid state. A low-frequency spectrum of electron oscillations consists of a low-frequency mode and split lines. We also show frequency controlling of the time evolution of an electron dipole moment on a phase shift between the two lasers. The low frequency can be increased or decreased, or it oscillates with the phase shift depending on the laser intensity.

I. INTRODUCTION

The response of an electron in double quantum wells to a strong laser field has been a subject of recent investigations.[1–14] In the case of no dissipation it has been shown numerically for two wells in Refs. 1–3 and analytically for two-level systems in Refs. 4–9 that an electron oscillates coherently between two states with a frequency Ω_0 that depends on a laser intensity

$$\Omega_0 = \Delta J_0(a), \tag{1}$$

where Δ is an energy between the two lowest subbands, and J_0 is the zeroth-order Bessel function. The parameter a is defined as

$$a \equiv \frac{2\mu_0 E_0}{\hbar\omega_0}, \tag{2}$$

where μ_0 is an electron dipole moment difference in the initial and final quantum states, E_0 and ω_0 are an amplitude and frequency of the cw laser field

$$E(t) = E_0 \cos(\omega_0 t). \tag{3}$$

At some values of the argument $J_0(a)=0$, i.e., $\Omega_0=0$. This means that the electron is trapped in one of the states. By changing the laser intensity a, the electron can be delocalized.

The effect of a dissipative environment changes a physical picture[10–14] qualitatively. In a cw field, electron density decays exponentially in time with the rate dependent on the laser parameters, electron-phonon coupling, the phonon spectrum, and the type of driving force. The intensity dependence of the rate constant is rather nonlinear exhibiting a resonance structure.[10,12] The reactant-product distribution function does not obey Gibbs law any longer. It can be manipulated by the field shifting equilibrium from products to reactants and vice versa independent of the bias.[12,13] Despite the strong electron-phonon interaction the electron oscillates between the states in a pulsed field giving rise to an induced coherence effect.[15,16]

In fact, in GaAs/Al_xGa_{1-x}As quantum wells dissipation is weak at low temperatures. This has been indirectly confirmed in experiments by observing quantum coherence of the electron in multiwell heterostructures.[17–20] The experimental observation of absolute negative resistance[21] predicted by Dakhnovskii and Metiu in Ref. 22 is also in favor of a weak dissipation mechanism at low temperatures. Indeed, under irradiation by a free electron laser, a negative current appears even when a positive voltage is applied (an ''anti-Ohm'' law). The theoretical prediction made has been based on the model where the interaction with phonons has been disregarded.[22] Thus, as a good approximated we will study electron dynamics in a nondissipative environment. Weak dissipation leads to coherent decay at low temperature while a pure exponential one is observable at high temperatures.[14] The effect of a weak field on electron coherence in a weakly interacting Ohmic bath has been considered recently by Makarov and Makri.[23]

In this work we study localization and delocalization of the electron in biased quantum wells where the interaction with the bath has been neglected. As mentioned above this is a good first approximation. We will show that electron dynamics is strongly determined by the ratio, $\epsilon/\hbar\omega_0$, of the bias energy, ϵ, and photon, $\hbar\omega_0$. In the case of symmetric double wells, electron tunneling and induced dipole moment behavior are considered in a bichromatic field. We demonstrate a nonanalytical dependence of localization conditions on a small incommensurability in the field frequencies. We

will also study how a low-frequency irradiation spectrum depends on a phase shift between the fields.

II. DELOCALIZATION GATES IN A PERIODICALLY DRIVEN BIASED TWO-LEVEL SYSTEM

We study localization and delocalization of an electron in a two-level system driven by a time-independent and a cw field. The time-dependent behavior of the electron in such fields is equivalent to dynamics in a biased two-level system driven by the periodic field.

The system is described by the following Hamiltonian:

$$\hat{H}=-\frac{\Delta}{\hbar}\sigma_x+V(t)\sigma_x, \tag{4}$$

where $V(t)$ is a driving force; σ_i $(i=x,y,z)$ are the Pauli matrices, and Δ is a transition matrix element (splitting of the lowest minibands). According to Ref. 24, the time-dependent probability may be defined as follows:

$$P(t)=\frac{1+x(t)}{2}, \tag{5}$$

where $x(t)=\langle\sigma_z(t)\rangle_{11}$; (11) is an 11 matrix element of σ_z. According to Ref. 4, one obtains the following master equation for the population difference

$$\frac{dx}{dt}=-\Delta^2\int_0^t dt_1\cos[F(t)-F(t_1)]x(t_1) \tag{6}$$

with the initial condition

$$x(t=0)=1, \tag{7}$$

where

$$F(t)\equiv 2\int_0^t dt_1 V(t_1). \tag{8}$$

The driving force consists of two parts: one is the constant field with the amplitude $\epsilon/2$, and the other is a periodic function with the frequency ω_0 and amplitude E_0

$$V(t)=\frac{\epsilon}{2}+\frac{\mu_0 E_0}{2}\cos(\omega_0 t), \tag{9}$$

where μ_0 is a dipole moment difference between the initial and final states. Thus $F(t)$ is equal to

$$F(t)=\epsilon t+a\ \sin(\omega_0 t), \tag{10}$$

$$a\equiv\frac{\mu_0 E_0}{\hbar\omega_0}. \tag{11}$$

Equation (6) may be presented in the equivalent integral form as follows:

$$x(\tau)=1-\left(\frac{\Delta}{\omega_0}\right)^2 \mathrm{Re}\int_0^\tau d\tau_1\exp[iF(\tau_1)] \times\int_0^{\tau_1} d\tau_2\exp[iF(\tau_2)]x(\tau_2). \tag{12}$$

Here we have introduced the following variable substitution:

$$\tau=\omega_0 t. \tag{13}$$

A solution of Eq. (12) is seeked as a perturbation expansion over the parameter $(\Delta/\omega_0)^2$, which is supposed to be small. Expanding the kernel of Eq. (6) into a Fourier series[25]

$$\exp\left[i\frac{\epsilon}{\hbar\omega_0}\tau+a\sin(\tau)\right]=\sum_{n=-\infty}^{\infty}J_n(a)\exp\left[i\left(\frac{\epsilon}{\hbar\omega_0}+n\right)\tau\right], \tag{14}$$

and assuming that the bias amplitude $\epsilon/\hbar\omega_0$ is close to a resonance with the photon energy $n_0\hbar\omega_0$, i.e.,

$$\left|\frac{\epsilon}{\hbar\omega_0}+n_0\right|\ll(|n_0|+1), \tag{15}$$

we collect only terms with the smallest denominators (15). Keeping only these resonance terms in an expression for the kernel, one finds that such a perturbation expansion can be generated by the following convolutive integrodifferential equation:

$$\frac{dx}{d\tau}=-\tilde{\Delta}^2\int_0^\tau d\tau_1\cos\left[\left(\frac{\epsilon}{\hbar\omega_0}+n_0\right)(\tau-\tau_1)\right]x(\tau_1), \tag{16}$$

where $\tilde{\Delta}$ denotes the renormalized tunneling splitting

$$\tilde{\Delta}\equiv\Delta J_{n_0}(a). \tag{17}$$

Equation (16) can be solved by a Laplace transform[26] with the initial condition (7)

$$x(\tau)=\frac{(\epsilon/\hbar\omega_0+n_0)^2}{w_n^2}+\frac{\tilde{\Delta}^2}{w_n^2}\cos(w_n\tau), \tag{18}$$

where w_n is defined as

$$w_n\equiv\sqrt{\tilde{\Delta}^2+(\epsilon/\hbar\omega_0+n_0)^2}. \tag{19}$$

At the exact resonance, when $|\epsilon|$ is equal to n_0 numbers of quanta

$$x(t)=\cos(\Delta J_{n_0}t). \tag{20}$$

In this case localization occurs when

$$J_{n_0}=0, \tag{21}$$

i.e., it is determined by zeros of the nth-order Bessel function. In fact, the approach developed may be generalized to an arbitrary periodic field with the period $2\pi/\omega_0$. By expanding the driving force $V(t)$ into a Fourier series

$$V(t)=\sum_{n=1}^{\infty}V_n\cos(n\omega_0 t), \tag{22}$$

and making use of the resonance method for the analysis of the power series for Eq. (12), one obtains a solution for the population difference that formally has the same form as in Eq. (18) with a renormalized tunneling matrix element defined as follows:

$$\tilde{\Delta}\equiv\Delta\sum_{m_1=-\infty}^{\infty}\cdots\sum_{m=-\infty}^{\infty}\cdots\prod_n J_m\left(\frac{2V_n}{n\hbar\omega_0}\right), \tag{23}$$

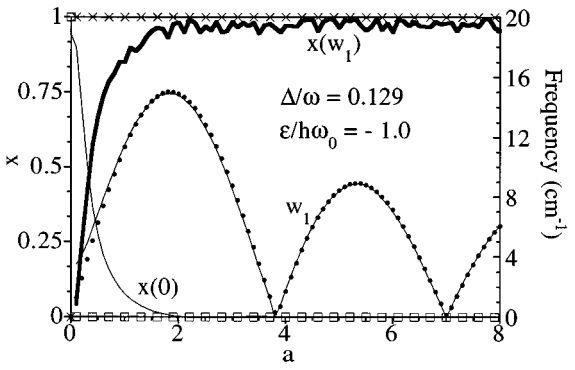

FIG. 1. The zero-frequency and the low-frequency components of the population difference (the induced dipole moment), $x(0)$ and $x(w_1)$ and the lowest-frequency w_1 as the function of a. The continuous lines are the numerical results. The values of w_1, $x(0)$, and $x(u_1)$ calculated using Eq. (18) as shown as dots, squares, and crosses, respectively. $\Delta=12.9\ \mathrm{cm}^{-1}$, $\omega_0=100\ \mathrm{cm}^{-1}$, $\epsilon/\hbar\omega_0=1$.

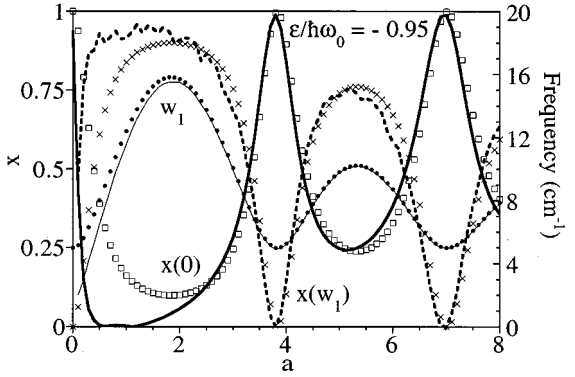

FIG. 2. The same as Fig. 1 except $\epsilon/\hbar\omega_0=0.95$.

where m_n satisfies the following condition:

$$\sum_n nm_n=m. \tag{24}$$

According to Eq. (18), $x(t)$ consists of two parts: one is a time-independent stationary part, and the other is an oscillatory part with the frequency w_n defined by Eq. (19). First of all, we have numerically tested the results described by Eq. (18) finding the Fourier transform $x(\omega)$, and plotting $|x(\omega)|$ as a function of ω. These plots have peaks whose heights give the amplitude of the Fourier component of x. We have found that as long as $\Delta/\omega_0\ll 1$ and $\epsilon/\hbar\omega_0=-n_0$, the zero frequency and the low frequency have the highest amplitudes, being in qualitative agreement with Eq. (18). For a quantitative test, in Fig. 1 we plot the amplitude of the zero-frequency-mode [denoted as $x(0)$], the amplitude of the low-frequency mode [denoted as $x(w_1)$], and the lowest-frequency w_1 as a function of the intensity parameter a. The numerical calculations were done for $\epsilon/\hbar\omega_0=1.00$ and $\Delta/\omega_0=0.125$. For these values Eq. (18) predicts $x(0)=0$, $x(w_1)=1$, and $w_1=\Delta/w_0J_1(a)$. We plot these predictions along with numerical results. As seen from Fig. 1, the analytical results are reasonable for $a>1$, and excellent for $a>2$. The intensity dependence of the low frequency agrees extremely well with the values obtained numerically, except at low intensities. Indeed, Eq. (19) predicts $w_1\to 0$ as $a\to 0$, while numerical results lead to a finite value. As the intensity of the laser field is increased, $x(0)$ becomes smaller while $x(w_1)$ increases. The sum of these two components is close to one. This means that the contribution from the other Fourier components is substantially suppressed, as predicted by the theory. The coherent motion of charge density leads to the intense low-frequency generation. The frequency varies with a and approaches zero as a gets close to the first zero of J_1. When $w_1=0$ (a=3.84) the low-frequency mode becomes static.

The theory makes predictions also for the case when $\epsilon/\hbar\omega_0$ is close to an integer. In Fig. 2 we compare the theory with numerical results for $\epsilon/\hbar\omega_0+n_0=-0.95$. As in the resonance case the agreement is rather good for $a>1$ and excellent for $a>2$. As the laser intensity is increased, the amplitude $x(0)$ of the static component is diminished but it never vanishes (as it does for $\epsilon/\hbar\omega_0=-1$) when a approaches the first zero (3.84) of J_1, $x(0)$ goes up to a maximum value. At this point the electron is completely localized as predicted by Eq. (18).

III. ELECTRON LOCALIZATION IN A TWO-LEVEL SYSTEM DRIVEN BY TWO FIELDS

In this section we study a response of an electron in a quantum double well driven by two lasers with frequencies ω_1 and ω_2. We show how two lasers are capable of manipulating electron localization and generating low-frequency radiation. Electron tunneling between two states is described by the Hamiltonian in Eq. (4). The time-dependent population difference obeys the kinetic integrodifferential equation (6) with initial condition (7). The electric field is given by

$$E(t)=E_1\cos(\omega_1 t)+E_2\cos(\omega_2 t). \tag{25}$$

Then $F(\tau)$ has the following form:

$$F(\tau)=a_1\sin(\tau)+a_2\sin[(1+\nu)\tau], \tag{26}$$

where a_i and ν are defined as

$$a_i\equiv\frac{\mu_0 E_i}{\hbar\omega_1}, \tag{27}$$

$$\nu\equiv\frac{\omega_2-\omega_1}{\omega_1}. \tag{28}$$

As discussed in the previous section, in the region where $(\Delta/\omega_1)^2\ll 1$, the solution of Eq. (6) or Eq. (12) may be analyzed via the perturbation expansion with respect to the small parameter $(\Delta/\omega_1)^2$. By making use of an expansion into a Fourier series[25]

$$\exp[iF(\tau)]=\sum_{n_1=-\infty}^{\infty}\sum_{n_2=-\infty}^{\infty}J_{n_1}(a_1)J_{n_2}(a_2)\times\exp\{[n_1+n_2(1+\nu)]\tau\}, \tag{29}$$

and after integrating of Eq. (12), one obtains a series of oscillating terms with amplitudes inversely proportional to their oscillating frequencies:

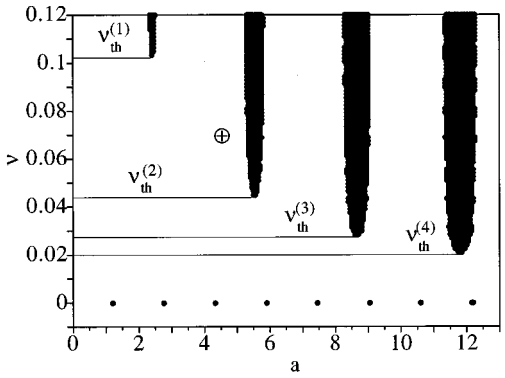

FIG. 3. The dark areas are localization regions in the parameter space $\{\nu,a_1\}$. $a_1=a_2$, $\Delta/\omega_1=0.1$, and $\omega_0=100\ \mathrm{cm}^{-1}$.

$$\frac{1}{[n_1+n_2(1+\nu)][n_3+n_4(1+\nu)]}. \tag{30}$$

Terms with the largest amplitudes satisfy the following conditions:

$$n_1+n_2=0,$$

$$n_3+n_4=0. \tag{31}$$

Picking up only the terms with the smallest denominators [satisfying condition (31)] in all orders of the perturbation expansion, one obtains the following solution:

$$x(t)=\cos\left(\frac{\Delta}{\omega_1}f(\tau)\right) \tag{32}$$

with

$$f(\tau)=\int_0^\tau J_0[\sqrt{a_1^2+a_1^2+2a_1a_2\cos(\nu\tau_1)}]. \tag{33}$$

If $\nu=0$ the system is driven by one laser with the electric field amplitude $E=E_1+E_2$ $(\omega_1=\omega_2=\omega)$. For this case

$$x(t)=\cos[\Delta J_0(a)t], \tag{34}$$

where a is defined by Eq. (27). If $J_0(a)=0$ the leading part of $x(t)$ becomes time independent and equals 1. This means that the electron is trapped in one of the wells.

We examine next what happens when the electron is driven by two lasers with $|\nu|\ll 1$. We define localization in one of the wells if

$$|x(\tau)|>0.95 \quad \text{for} \quad \tau<500. \tag{35}$$

This condition requires the electron to be localized within 95%. Complete localization means that $x(\tau)=1$ at all times. Since $x(\tau)$ depends on the parameters a_1, a_2, and Δ/ω_1, we will now explore this multiparameter space selectively. In Fig. 3 the dark regions show the parameter values in the $\{\nu,a_1\}$ plane, for which localization condition (35) is satisfied. The results for negative values of ν are symmetrical to those for positive ν. Since $\nu=0$ means that only one laser acts, the points along the ν axis are given by the condition $|\cos[\Delta J_0(a)t]|>0.95$ for $\tau<500$. This gives small regions centered around the roots of the equation $J_0(a)=0$. If we change 0.95 to a larger number (but less than 1) or take τ to longer times, the area will shrink.

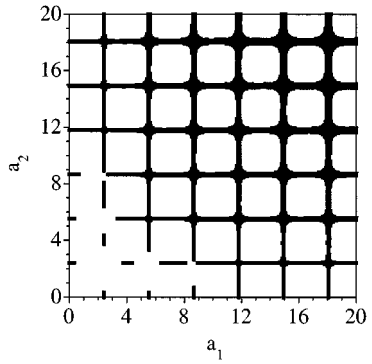

FIG. 4. The dark areas are localization regions in the parameter space $\{a_1,a_2\}$. $\nu=0.1$, $\Delta/\omega_1=0.1$, and $\omega_0=100\ \mathrm{cm}^{-1}$.

The fact that for $\nu=0$ electron localization takes place is not surprising (see Refs. 4, 5, and 8). However, the ''fingers'' appearing in the upper part of Fig. 3 for larger values of ν are unexpected. These regions are not continuously connected to the circles on the $\nu=0$ lines. This means that a perturbation over small ν fails, i.e., $x(t)$ is a nonanalytical function of ν. It can be clearly seen from the following substitution:

$$\tilde{\tau}=\nu\tau. \tag{36}$$

Then

$$x(\tilde{\tau})=\cos\left[\frac{1}{\nu}\left(\frac{\Delta}{\omega_1}\right)f(\tilde{\tau})\right]. \tag{37}$$

For longer times, where $\tilde{\tau}\gg 1$ when $\nu\to 0$, $x(t)$ is a nonanalytical function of ν.

In Fig. 4 we demonstrate localization regions in the plane $\{a_1,a_2\}$. They form strips lined up along the zeros of the Bessel function J_0. The larger the field intensity, the thicker the localization regions.

In Fig. 5 we show the low-frequency part of the Fourier transform of $x(t)$. We give only the peak heights and positions. The parameters for which the spectrum has been cal-

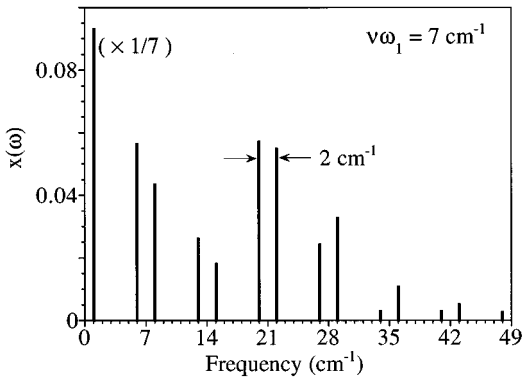

FIG. 5. The low-frequency part of the Fourier spectrum of the induced dipole for the point in the parameter space marked by ''+'' in Fig. 3. $a_1=a_2=4.5$, $\Delta/\omega_1=0.1$, and $\nu=0.07$. The spectrum has peaks at $n\nu\pm\delta$, where $\delta=1\ \mathrm{cm}^{-1}$.

culated correspond to the cross in Fig. 3, which is a point inside the "finger." Figure 5 shows a low-frequency harmonic, δ, located near $\omega=0$ ($\delta=1$ cm^{-1}), and demonstrates new harmonics at the frequencies $n(\omega_1-\omega_2)\pm\delta$. As the parameters approach to the region of localization, δ becomes smaller and ultimately vanishes; furthermore the shifted harmonics get closer and eventually collapse.

The low-frequency part of the spectrum can be understood from Eq. (33). Indeed, $f(\tau)$ given by Eq. (33) can be expanded as[25]

$$f(\tau)=J_0(a_1)J_0(a_2)\tau+\sum_{n=-\infty}^{\infty} a_n\frac{\sin(n\nu\tau)}{n\nu} \tag{38}$$

with

$$a_n\equiv 2(-1)^n J_n(a_1)J_n(a_2). \tag{39}$$

The leading term in Eq. (38) is

$$\delta\tau\equiv J_0(a_1)J_0(a_2)\tau, \tag{40}$$

which grows [when $J_0(a_1)J_0(a_2)\neq 0$] indefinitely in time, while the other terms are restricted. Moreover the amplitude of $J_n(a_1)J_n(a_2)/n\nu$ is small compared to τ. Inserting (38) into Eq. (32) and making use of $\cos(a+b)=\cos a\cos b-\sin a\sin b$ repeatedly retaining the largest term, the one containing cosines only (the terms containing sines are small with respect to the small parameter Δ/ω_1), we obtain

$$\cos\left[\left(\frac{\Delta}{\omega_1}\right)f(\tau)\right]\simeq\cos(\delta\tau)\cos\left(a_1\frac{\sin(\nu\tau)}{\nu}\right)\cdots \times\cos\left(a_n\frac{\sin(n\nu\tau)}{n\nu}\right)\cdots . \tag{41}$$

Using in this and the formula[25]

$$\cos\left(a_n\frac{\sin(n\nu\tau)}{n\nu}\right)=J_0\left(\frac{a_n}{n\nu}\right)+2\sum_{m=1}^{\infty}J_{2m}\left(\frac{a_n}{n\nu}\right)\cos(mn\nu\tau), \tag{42}$$

we obtain the Fourier components of $x(t)=\cos[(\Delta/\omega_1)f(\tau)]$. We show here only a few first terms

$$x(\tau)=\prod_{n=1}^{\infty}J_0(a_n)\cos(\delta\tau)+\frac{1}{2}J_1(a_1)\prod_{n=2}^{\infty}J_0(a_n) \times\{\cos[(\delta+\nu)\tau]+\cos[(\delta-\nu)\tau]\}+\cdots . \tag{43}$$

This equation is not exact, it is a perturbative series, where neglected terms are of the order of $(\Delta/\omega_1)^2$. For this reason the formula does not contain the higher-frequency components of $x(\tau)$ such as, for example, the shifted harmonics at the frequencies $n\omega_1$. The formula predicts that the amplitudes of the terms with the frequencies $\delta+\nu$ and $\delta-\nu$ are equal. The numerical results shown in Fig. 5 give nearly equal intensities as predicted.

Taking the limit $\nu\to 0$ in Eq. (38), which corresponds to one laser with the intensity parameter $a=a_1+a_2$, leads to

$$f(\tau)\to\left\{J_0(a_1)J_0(a_2)+2\sum_{n=1}^{\infty}(-1)^n J_n(a_1)J_n(a_2)\right\}\tau=J_0(a)\tau. \tag{44}$$

IV. PHASE-DEPENDENCE STARK SHIFT IN A TWO-LEVEL SYSTEM DRIVEN BY TWO LASERS

In this section we investigate the role of laser phases when the electron-photon interaction is strong. Some phase dependence of observable processes has been already found in such systems. Potvliege and Smith[27] have shown that the ionization rate of the hydrogen atom is affected by the relative phase driving the system. Bavli and Metiu[2] have pointed out that the ability of the laser to maintain electron localization is weakly dependent on the phase. If the electric field of the laser has a time dependence $\cos(\omega t+\phi)$ the transformation $t\to t'-\phi/\omega$ changes $\partial t\to\partial t'$, $\cos(\omega t+\phi)\to\cos(\omega t')$. Thus a shift in the origin of the time scale eliminates phase from a time-dependent Schrödinger equation. Nevertheless calculations[2] showing that the probability of finding the electron driven by one laser in a given well depends on ϕ are not erroneous. In these calculations the electron was localized in one well at $t=0$, and this initial state, being a coherent superposition of eigenstates, changes when the time scale is shifted. For example, for a two-level system whose energies with no laser field are ϵ_1 and ϵ_2, the initial state $|1\rangle+|2\rangle$ at $t=0$ changes to $\exp[i\phi\epsilon_1/\hbar\omega]|1\rangle+\exp[i\phi\epsilon_2/\hbar\omega]|2\rangle$. Since the initial condition is an intrinsic part of a well formulated physical problem the solution of the Schrödinger equation depends on ϕ.

The situation is more interesting when the system is driven by two lasers. The electric field of the two lasers, having frequency ω and $p\omega$ (p is an integer) is

$$E(t)=E_1\cos(\omega t+\phi_1)+E_2\cos(p\omega t+\phi_2). \tag{45}$$

The time scale changes $t\to t'-\phi/\omega$ lead to the electric field $E_1\cos(\omega t')+E_2\cos(p\omega t+\phi_2-p\phi_1)$. The Hamiltonian depends on the parameter $\phi(p)=\phi_2-p\phi_1$ and, therefore, the energies controlling the time evolution of the wave function will also depend on $\phi(p)$. By using the method applied for the derivation of Eqs. (32) and (33) we obtain that low-frequency Ω is determined by the following equation:

$$\Omega/\omega=J_0(a_1)J_0(a_2) +2\sum_{n=0}^{\infty}(-1)^n J_{np}(a_1)J_n(a_2)\cos[\phi(p)]. \tag{46}$$

This equation is valid when $\Delta/\omega\ll 1$. This result is derived by expanding the equation of motion in powers of Δ/ω and resuming the fastest growing secular terms. In Fig. 6 we compare the low frequency calculated numerically to that

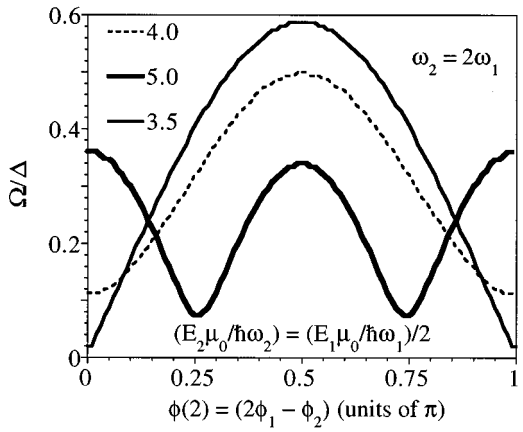

FIG. 6. The frequency Ω of the slow mode of the induced dipole as a function of the phase parameter $\phi(2)=\phi_2-2\phi_1$. The laser frequencies are ω and 2ω, $E_1=E_2$, and $\Delta/\omega_1=0.1$.

predicted analytically by Eq. (46), and find excellent agreement. The phase parameter $\phi(p)$ is chosen for $p=2$. For $a_1=3.5$ and $a_2=a_1/2$ the low-frequency Ω varies by a factor of 60. The frequency has always a maximum at $\phi(2)=\pi/2$. As shown in Fig. 6, Ω can oscillate with respect to ϕ ($a_2=5.0$). At this laser intensity the frequency can be even lower than the value with no phase shift. As shown in Fig. 7, localization can be reached by changing the phase difference even if the electron has not been localized by the field with no phase shift. Localization regions and the character of the phase dependence of the low frequency is determined by the laser intensity.

Localization regions (over 90% of the electron density is in the initial state) are shown by the dark lines in Fig. 8 when $\omega_2=3\omega_1$ and $E_2=E_1$. The inclusion of the phase between the fields can increase an area of localization. A few examples given above make it clear that the phase parameter $\phi(p)$ has a substantial influence on all properties of the driven electron. It effects not only the amplitude (as in the case of a weak field) but also the frequency with which the electron responds to the laser.

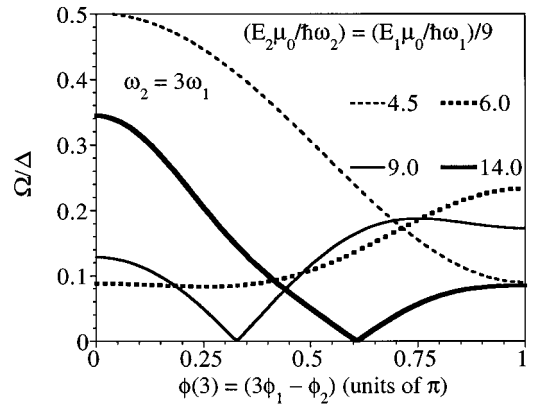

FIG. 7. The frequency Ω of the slow mode of the induced dipole as a function of the phase parameter $\phi(3)=3\phi_1-\phi_2$. The laser frequencies are ω and 2ω, $E_2=E_1/3$, and $\Delta/\omega_1=0.1$.

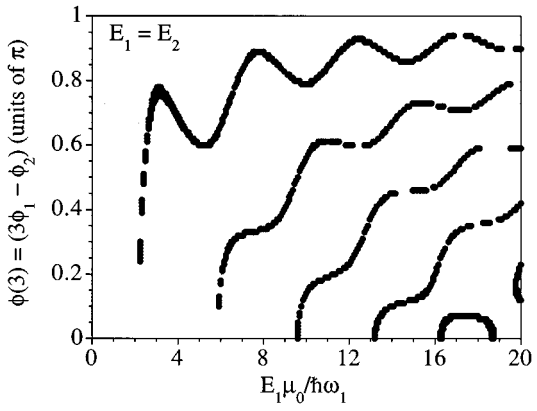

FIG. 8. The dark regions indicate that the value of $\phi(3)=3\phi_1-\phi_2$ and a for which 90% of the electron density is in the left well. $E_2=E_1$, $\omega_2=3\omega_1$.

V. CONCLUSIONS

We have considered the effect of a strong electric field on an electron injected into a quantum well for different types of electric fields and different types of quantum wells including biased ones.

If the electron is initially localized in one of the biased wells (the lowest one) it can be delocalized by an electric field if the bias energy is close to an integer number photon energy (but not equal to), $\epsilon \equiv n_0\hbar\omega_0$. Localization takes place again when the field is an exact resonance with the bias. This localization is determined by a different physical reason, it is dynamical localization. The intensity of the field is determined by the zeros of $J_{n_0}(a)$, where n_0 is the number of absorbed (emitted) photons.

When the mismatch between the photon energy and the bias is small, the electron oscillates between the wells with the frequency determined by both the mismatch and the splitting renormalized by the Bessel function of the n_0th order [Eq. (18)]. Analytical predictions were verified by exact numerical calculations. The results have been generalized to an arbitrary periodic field.

In Sec. III we considered localization conditions and a low-frequency generation for the electron driven by a bichromatic field in a case when two frequencies are very close to each other. At $\nu=(\omega_2-\omega_1)/\omega_1=0$ the electron is localized under conditions valid for the single field case. As ν is increased localization is no longer possible until higher values of $\nu_{\rm th}$ are reached; then localization is possible again in the extended regions of the parameter space (see Fig. 3). These regions cannot be obtained from a simple power expansion with $\nu \ll 1$. A population difference between the states is a nonanalytical function of ν [see Eq. (37)]. Such behavior is rather common in the physics of phase transitions where correlation functions behave nonanalytically in the vicinity of a transition point. The low-frequency spectrum has been studied as well. Figure 5 shows that a spectrum consists of a low frequency and harmonics at the frequencies $n(\omega_1-\omega_2)\pm\delta$. As the parameters approach to a region of localization, δ becomes smaller and smaller and ultimately vanishes; furthermore, the shifted harmonics get closer and eventually collapse (see Fig. 5).

If there is a phase shift between the fields only an ampli-

tude change is expected in an electron response when a weak field is applied. However, as shown in Sec. IV, it is not so for the strong fields. The phase shift affects a low-frequency spectrum. The low frequency can be increased by 2 orders of magnitude for the intensity $a_1=3.5$ ($a_2=a_1/2$). However, for $a_1=5.0$ it can be lowered by a factor of 3 (see Fig. 6). Moreover, the low frequency can oscillate with ϕ. As shown in Fig. 7, the electron can even be trapped by changing the phase shift only keeping the intensity to be unchanged.

A two-level model considered in this work implies that ionization by a static field and multiphoton absorption is neglected. Indeed, if the photon energy is rather small ($\sim 50-80$ cm^{-1}) it needs 50–30 quanta to reach a continuum spectrum for the typical value of barrier height of $V_g \simeq 0.3$ eV for $Al_xGa_{1-x}As/GaAs$.[28] In this paper we consider rather weak fields when only 2–5 quanta are absorbed. For the barrier width of 50 Å, ionization induced by the static field begins when $\mu_0 \epsilon = V_g$, i.e., the amplitude of the field should be less than 6×10^5 V/cm. Thus for such static and alternative fields, ionization can be disregarded.

ACKNOWLEDGMENTS

This work was supported by NSF CHE 91-12926. We are grateful to Rob Coalson, Debi Evans, Jim Allen, and H.M. to Martin Holthaus for helpful discussions.

[1] F. Grossmann, T. Dittrich, P. Jung, and P. Hänggi, Phys. Rev. Lett. **67**, 561 (1991); F. Grossmann, T. Dittrich, and P. Hänggi, Physica B **175**, 293 (1991); F. Grossmann, T. Dittrich, P. Jung, and P. Hänggi, Z. Phys. B **85**, 315 (1991); F. Grossmann and P. Hänggi, Europhys. Lett. **18**, 571, (1992); T. Dittrich, P. Öelschlagel, and P. Hänggi, *ibid.* **18**, 571 (1993).

[2] R. Bavli and H. Metiu, Phys. Rev. Lett. **69**, 1986 (1992); Phys. Rev. A **47**, 3299 (1992).

[3] W. A. Lin and L. E. Ballentine, Phys. Rev. Lett. **65**, 2927 (1990).

[4] Yu. Dakhnovskii and H. Metiu, Phys. Rev. A **48**, 2342 (1993); Yu. Dakhnovskii and R. Bavli, Phys. Rev. B **48**, 11 010 (1993); **48**, 11 020 (1993); Phys. Rev. A **48**, R886 (1993).

[5] M. Yu. Ivanov, P. Corcum, and P. Dietrich, Laser Phys. **3**, 375 (1993).

[6] J. M. Gomez Llorente, and P. Plata, Phys. Rev. A **45**, R6958 (1992).

[7] D. Farrely and J. A. Milligan, Phys. Rev. E **47**, R2225 (1993).

[8] T. Zuo, S. Chelkowski, and A. Bandrauk, Phys. Rev. A **49**, 3943 (1994); N. Ben-Tal, N. Moiseyev, and R. Kosloff, J. Chem. Phys. **98**, 9610 (1993); K. Schafer and K. Kulander, Phys. Rev. A **45**, 8026 (1992).

[9] Yu. Dakhnovskii and R. Bavli, J. Phys. Chem. **67**, 561 (1994).

[10] Yu. Dakhnovskii, J. Chem. Phys. **100**, 6492 (1994).

[11] M. Morillo and R. I. Cukier, J. Chem. Phys. **98**, 4548 (1993); Chem. Phys. **183**, 375 (1994).

[12] Yu. Dakhnovskii and R. D. Coalson, J. Chem. Phys. **103**, 2908 (1995).

[13] Yu. Dakhnovskii, D. G. Evans, H. Kim, and R. D. Coalson, J. Chem. Phys. **103**, 5461 (1995).

[14] Yu. Dakhnovskii, Ann. Phys. (N.Y.) **229**, 145 (1994).

[15] D. G. Evans, R. D. Coalson, H. Kim, and Yu. Dakhnovskii, Phys. Rev. Lett. **75**, 3649 (1995).

[16] D. G. Evans, R. D. Coalson, and Yu. Dakhnovskii, J. Chem. Phys. (to be published).

[17] K. Leo, J. Shah, E. O. Göbel, T. C. Dame, S. Schmitt-Rink, W. Schafäfer, and K. Kölher, Phys. Rev. Lett. **66**, 201 (1991).

[18] H. G. Roskos, M. C. Nuss, J. Shah, K. Leo, D. A. B. Miller, A. M. Fox, S. Schmitt-Rink, and K. Kölher, Phys. Rev. Lett. **68**, 2216 (1992).

[19] M. S. Luo, S. L. Chuang, P. C. M. Planken, I. Brener, and M. Nuss, Phys. Rev. B **48**, 11 043 (1993).

[20] I. Brener, P. C. M. Planken, M. Nuss, L. Pfeiffer, D. E. Leard, and A. M. Weiner, Appl. Phys. Lett. **63**, 2213 (1993).

[21] B. J. Keay, S. J. Allen, Jr., J. P. Kaminski, J. Galan, K. L. Campman, A. C. Gossard, U. Bhattacharaya, and M. J. M. Rodwell (unpublished).

[22] Yu. Dakhnovskii and H. Metiu, Phys. Rev. B **51**, 4193 (1995).

[23] D. Makarov and N. Makri, Phys. Rev. B **52**, R2257 (1995).

[24] S. Chakravarty and A. Leggett, Phys. Rev. Lett. **52**, 5 (1984); A. Leggett, S. Chakravarty, A. T. Dorsey, M. P. A. Fisher, A. Garg, and W. Zwerger, Rev. Mod. Phys. **59**, 1 (1987).

[25] I. S. Gradstein and I. M. Ryzhik, *Tables of Integrals, Series, and Products* (Academic, New York, 1980).

[26] *Handbook of Mathematical Functions*, edited by M. Abramowitz and I. A. Stegun, Natl. Bur. Stand. (U.S.) Appl. Math. Ser. No. 55 (U.S. GPO, Washington, D.C., 1964).

[27] A. M. Potvliege and P. H. G. Smith, J. Phys. B **24**, L641 (1991).

[28] G. Bastard, J. A. Brum, and R. Ferreira, in *Solid State Physics*, edited by H. Ehrenreich and D. Turnbull (Academic, New York, 1991), Vol. 44, p. 229.